Autocrine Function of Aldehyde Dehydrogenase 1 as a Determinant of Diet- and Sex-Specific Differences in Visceral Adiposity

Rumana Yasmeen,[1] Barbara Reichert,[1] Jeffrey Deiuliis,[2] Fangping Yang,[1] Alisha Lynch,[1] Joseph Meyers,[1] Molly Sharlach,[3] Sangsu Shin,[4] Katharina S. Volz,[1] Kari B. Green,[5] Kichoon Lee,[4] Hansjuerg Alder,[6] Gregg Duester,[7] Rudolf Zechner,[8] Sanjay Rajagopalan,[2] and Ouliana Ziouzenkova[1]

Mechanisms for sex- and depot-specific fat formation are unclear. We investigated the role of retinoic acid (RA) production by aldehyde dehydrogenase 1 (Aldh1a1, -a2, and -a3), the major RA-producing enzymes, on sex-specific fat depot formation. Female *Aldh1a1*$^{-/-}$ mice, but not males, were resistant to high-fat (HF) diet–induced visceral adipose formation, whereas subcutaneous fat was reduced similarly in both groups. Sexual dimorphism in visceral fat (VF) was attributable to elevated adipose triglyceride lipase (Atgl) protein expression localized in clusters of multilocular uncoupling protein 1 (Ucp1)-positive cells in female *Aldh1a1*$^{-/-}$ mice compared with males. Estrogen decreased *Aldh1a3* expression, limiting conversion of retinaldehyde (Rald) to RA. Rald effectively induced Atgl levels via nongenomic mechanisms, demonstrating indirect regulation by estrogen. Experiments in transgenic mice expressing an RA receptor response element (RARE-lacZ) revealed HF diet–induced RARE activation in VF of females but not males. In humans, stromal cells isolated from VF of obese subjects also expressed higher levels of *Aldh1* enzymes compared with lean subjects. Our data suggest that an HF diet mediates VF formation through a sex-specific autocrine Aldh1 switch, in which Rald-mediated lipolysis in Ucp1-positive visceral adipocytes is replaced by RA-mediated lipid accumulation. Our data suggest that Aldh1 is a potential target for sex-specific antiobesity therapy. ***Diabetes*** **62:124–136, 2013**

From the [1]Department of Human Nutrition, The Ohio State University, Columbus, Ohio; the [2]Davis Heart and Lung Research Institute, The Ohio State University, Columbus, Ohio; the [3]Department of Plant and Microbial Biology, University of California, Berkeley, Berkeley, California; the [4]Department of Animal Sciences, The Ohio State University, Columbus, Ohio; the [5]Mass Spectrometry and Proteomics Facility, The Ohio State University, Columbus, Ohio; [6]Nucleic Acid Shared Resource, Comprehensive Cancer Center, The Ohio State University, Columbus, Ohio; the [7]Development and Aging Program, Sanford-Burnham Medical Research Institute, La Jolla, California; and the [8]Institute of Molecular Biosciences, Karl Franzens University, Graz, Austria.

Corresponding author: Ouliana Ziouzenkova, ziouzenkova.1@osu.edu.

Received 20 December 2011 and accepted 30 June 2012.

DOI: 10.2337/db11-1779

This article contains Supplementary Data online at http://diabetes.diabetesjournals.org/lookup/suppl/doi:10.2337/db11-1779/-/DC1.

R.Y. and B.R. contributed equally to this work.

The content is solely the responsibility of the authors and does not necessarily represent the official views of the National Institute of Diabetes and Digestive and Kidney Diseases or the National Institutes of Health.

The higher prevalence rates of obesity in women (61.3 vs. 42% prevalence in men) correlate with a higher risk for type 2 diabetes, cardiovascular disease, cancer, and premature death (1–4). The onset of adiposity occurs on a Western diet in premenopausal women (5,6) or after menopause (7). On a regular diet, preferential distribution of fat to visceral depots is atypical for females but occurs in males (8). Obesity is a polygenic and multifactorial disorder with various predisposing factors, including sex hormones and obesogenic diets (9). The effector mechanisms modulating visceral fat (VF) accumulation in females and, in particular, their relationship to high-fat (HF) diets are poorly characterized (9,10).

Vitamin A metabolites retinaldehyde (Rald) and retinoic acid (RA) regulate cell differentiation and metabolism in adipose and other tissues (11). RA is a high-affinity RA receptor (RAR) ligand (12). Activated RAR and retinoid X receptor (RXR) complexes bind to RA response elements (RARE) and regulate target gene expression (13). RA influences numerous other transcription pathways, including peroxisome proliferator–activated receptor γ (PPARγ), the master regulator of adipogenesis, C/EBP, PPARδ, and Smad3 (reviewed in Ref. 11). The RA effects on adipogenesis are concentration-dependent. Low-autocrine RA generation by the cytosolic aldehyde dehydrogenase 1 (Aldh1a1, -a2, and -a3) enzyme family (14) stimulates adipogenesis via mechanisms dependent on transcription factors ZFP423 and PPARγ (15). In humans, therapeutic RA doses can cause RA syndrome demonstrating increased adiposity (16). Conversely, rodents respond to administration of high RA doses with obesity suppression by RAR, C/EBP, PPARδ, Krueppel-like factor 2, and/or Smad3 pathways (11,17,18) and possible repression of the autocrine Aldh1a1 pathway in adipocytes (15) and the liver (19). Rald is the unique precursor of RA (14), which represses adipogenesis by inhibiting RXR and PPARγ (20). A recent study (21) showed that both RA and Rald regulated uncoupling protein 1 (Ucp1) expression through RAR in vitro, with Rald being a weaker RAR ligand than RA (21,22). However, the relevance of this finding is unknown because only *Aldh1a1*$^{-/-}$ female mice developed thermogenic adipocytes in white fat, whereas wild-type (WT) mice expressing all RA-generating enzymes Aldh1a1, -a2, and -a3 maintained low Ucp1 levels and remained obese.

RA is produced primarily by Aldh1a1 in VF and by Aldh1a1 and Aldh1a3 in subcutaneous fat (15). In consonance with their tissue-specific distribution, *Aldh1a1*$^{-/-}$

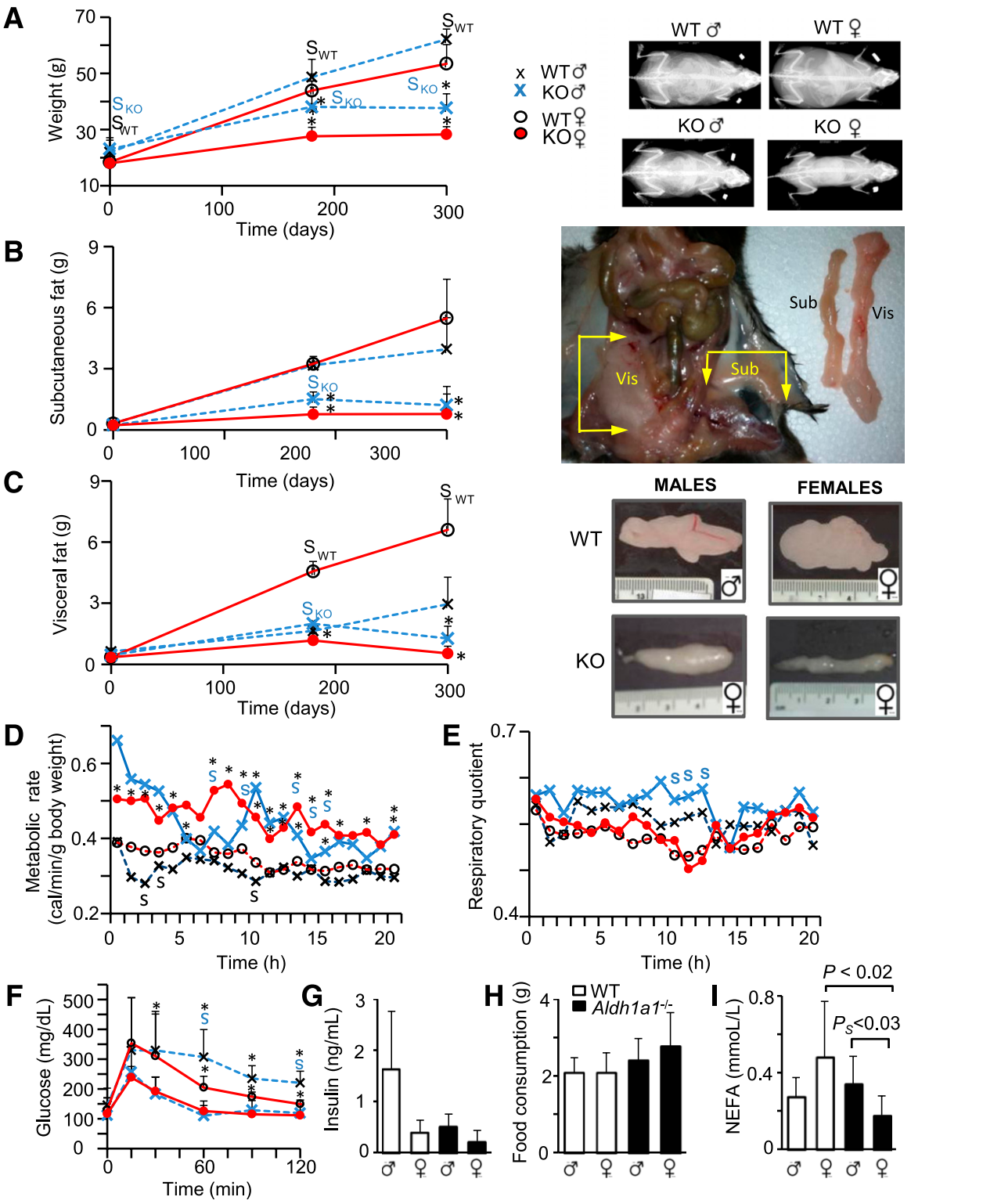

FIG. 1. Deficiency in *Aldh1a1* suppresses fat accumulation in response to HF feeding in a depot- and sex-specific manner. *A*: Whole-body weights are shown in WT (males, small black X, $n = 18$; females, open circles, $n = 17$) and *Aldh1a1*$^{-/-}$ (males, large blue X, $n = 18$; females, closed red circles, $n = 23$) on RC; in WT (males, $n = 8$; females, $n = 9$) and *Aldh1a1*$^{-/-}$ (males, $n = 9$; females, $n = 11$) mice on an HF diet for 180 days; and in WT (males, $n = 7$; females, $n = 9$) and *Aldh1a1*$^{-/-}$ (males, $n = 9$; females, $n = 9$) mice for 300 days. *$P < 0.001$ differences between genotypes; S_{WT} (black) or knockout (KO; blue), differences between sexes within one genotype. X-ray images showed randomly selected mice from each group on a regular and HF diet for 180 days. Subcutaneous (*B*) and visceral (perigonadal) (*C*) fat pads were dissected as shown in the insets at *right*: WT (males, $n = 9$; females, $n = 8$) and *Aldh1a1*$^{-/-}$ (KO; males, $n = 9$; females, $n = 8$) on RC; in WT (males, $n = 5$ and females, $n = 5$) and in *Aldh1a1*$^{-/-}$ (males, $n = 4$; females, $n = 4$) mice on an HF diet for 180 days; in WT (males, $n = 7$; females, $n = 9$) and *Aldh1a1*$^{-/-}$ (males, $n = 9$ and females, $n = 9$) mice for 300 days. *$P < 0.001$ differences between genotypes in the same sex-group; SDifferences between sexes within one genotype. Images show one VF pad dissected from randomly selected WT and KO male and female mice that consumed an HF diet for 180 days. Metabolic rate (*D*) and RQ (*E*) in WT (dashed line, males [blue X, $n = 4$] and females [red circles, $n = 5$]) and *Aldh1a1*$^{-/-}$ (solid line, males [$n = 3$] and females [$n = 5$]). Data were calculated [Weir equation (50)] based on food and oxygen consumption as well as CO_2 release in metabolic cages. *$P < 0.05$ differences between genotypes; P_S, $P < 0.05$, differences between sexes within one genotype (black font, WT; blue font, KO). Mann-Whitney *U* test (for panels *D–F*).

mice develop less VF than subcutaneous fat when compared with WT mice on a regular diet (11,15). HF diet in the liver and estrogen in the uterus induced *Aldh1* expression in mice, possibly directly through estrogen receptor sites in the promoter of Aldh1a2 and sterol regulatory element–binding protein sites in the promoter of Aldh1a1 and Aldh1a2 (23–25). We hypothesized that adipose tissue responds to HF feeding or sex hormones by intrinsic RA production. In this study, we provide evidence of sex- and depot-specific increases in RA generation and dysregulation of Aldh1 in mouse and human adipose.

RESEARCH DESIGN AND METHODS

Reagents. We purchased reagents from Sigma-Aldrich (St. Louis, MO) and cell-culture media from Invitrogen (Carlsbad, CA) unless otherwise indicated. Adipose triglyceride lipase (Atgl) and glyceraldehyde-3-phosphate dehydrogenase antibodies were from Cell Signaling Technology (Danvers, MA); Ucp1, β-actin, and tubulin were from Abcam (Cambridge, MA); and secondary antibodies were from LI-COR Biosciences (Lincoln, NE). 17-β-Estradiol was obtained from Cayman Chemical (Ann Arbor, MI), and ELISA kits for E2 and insulin were from Abnova (Walnut, CA) and Millipore (Billerica, MA). All-*trans* retinoids were stored under argon and protected from light.

Human studies. VF was obtained from the greater omentum during endoscopic repair of hernias from overnight fasted lean subjects (BMI <30) and bariatric surgeries (laparoscopic banding and gastric bypass) in obese patients (BMI ≥40). Institutional review board–approved informed consent was obtained for the patients' medical records. Stromal vascular fraction (SVF) was isolated from VF using Ficoll-Hypaque (GE Healthcare) as described (26).

Animal studies. Animal studies were approved by the Institutional Animal Care and Use Committee.

Study 1. *Aldh1a1*$^{-/-}$ mice were constructed by Duester and colleagues (27) and initially characterized by Reichert et al. (15) and Ziouzenkova et al. (20). Age- (8 weeks old) and sex-matched C57BL/6J (WT) and *Aldh1a1*$^{-/-}$ mice were fed either a regular chow (RC) or HF diet (45% kcal from fat with standard 4 IU vitamin A/g; D12451; Research Diets Inc., New Brunswick, NJ) for 180 and 300 days, respectively. Food intake and metabolic rate were measured after mouse acclimation to a powdered HF diet (4 days) in metabolic cages (Ancare; Charles River Laboratories).

Study 2. Seven-month-old WT and *Aldh1a1*$^{-/-}$ females were ovariectomized or sham operated. Mice continued on an RC diet for 3 months after surgery.

Study 3. Three-month-old Tg(RARE-Hspa1b/lacZ)12Jrt/J (denoted as RARE-lacZ) mice were purchased from JAXmice (Bar Harbor, ME). These mice were developed by Dr. Rossant using a transgenic construct containing three copies of the 32-bp RARE placed upstream of the mouse heat shock protein 1B promoter and β-galactosidase gene (lacZ) (28). Two RARE-lacZ mouse groups received RC or an HF diet (same as in study 1) for 150 days. In all animal studies, weight and food consumption were measured weekly.

Glucose tolerance test. A glucose tolerance test (GTT) was performed in overnight fasted mice by intraperitoneal injection of 0.004 mL 25% glucose/g body weight.

Cell culture. Murine NIH3T3-L1 (3T3-L1) preadipocytes were cultured and differentiated using standard procedures (20). Preadipocytes differentiated for 7–12 days were denoted as mature and stimulated in ultraviolet (UV)-treated FBS depleted of retinoids. Human Simpson-Golabi-Behmel syndrome (SGBS) preadipocytes were cultured and differentiated in Dulbecco's modified Eagle's medium (DMEM)/Ham's F12 containing 10% FBS as described (29). Nonesterified fatty acids (NEFA) were measured in media at 45 min and 3 h using a NEFA-HR kit (Wako Diagnostics, Richmond, VA).

SVF. SVF was isolated from VF of 16- and 11-month-old WT and *Aldh1a1*$^{-/-}$ female mice, respectively, on an RC diet as described (30).

Explant cultures. VF was isolated from three *Aldh1a1*$^{-/-}$ or RARE-lacZ males fed RC. Each fat pad was excised into four equal-by-weight sections for stimulation with retinoids (~87 mg/fat section, 5 mL 1% UV-treated FBS DMEM/g fat). Explants were stimulated with isoproterenol (10 μmol/L) in DMEM containing 2% fatty acid-free BSA (Sigma-Aldrich) (5 mL medium/g fat). Medium was collected every 30 min for 2 h for NEFA detection. Other explants were homogenized in radioimmunoprecipitation assay buffer containing protease inhibitors (Roche, Indianapolis, IN) or used for mRNA isolation.

Western blot. Cell/tissue lysates normalized by protein content were separated on 10% acrylamide gel under reducing conditions, transferred to a polyvinylidene fluoride membrane (Immobilon-P; Millipore). Proteins were analyzed using an Odyssey Infrared Imaging System (LI-COR Biosciences).

Proteomic two-dimensional fluorescence difference gel electrophoresis. Four radioimmunoprecipitation assay homogenates each from VF of males and females of WT and *Aldh1a1*$^{-/-}$ genotypes were precipitated with 10% trichloroacetic acid and used for two-dimensional fluorescence difference gel electrophoresis (DIGE; GE Healthcare). Samples were labeled with DIGE fluor minimal-label dyes and focused on 18-cm (pH 4–7) Immobiline strips using an IPGphor II IEF (GE Healthcare). After SDS-PAGE, individual gels were spot mapped using an internal standard. An independent *t* test ($P < 0.05$) between WT and *Aldh1a1*$^{-/-}$ groups in males and females was performed to identify spots with >1.5-fold differences in abundance with spots appearing in at least three of the four gels. Significantly changed spots were cored from preparative gels (Ettan workstation) and identified using an LTQ mass spectrometer detector (Thermo Scientific).

Histology. VF embedded in paraffin was stained with Atgl or Ucp1 polyclonal rabbit antibodies (1:1,000 dilution).

Semiquantitative mRNA analysis. cDNA was prepared from purified mRNA (Qiagen, Valencia, CA) and analyzed using a 7900HT Fast Real-Time PCR System, TaqMan detection system, and validated primers (Applied Biosystems, Foster City, CA) in triplicate, including no-template controls. The mRNA expression was calculated based on 18S expression using the threshold cycle method. The β-galactosidase assay was designed based on GenBank: U46489.1 standard LacZ (22 bp, underlined) surrounded by 50 bp (Applied Biosystems probe design): 5′-GCCGATACTGTCGTCGTCCCCTCAAACTGGCAGATGCACGGTTACGATGCGCCCATCTACACCAACGTAACCTATCCCATTACGGTCAATCCGCCGTTTGTTCCCACGGAGAATCCGACGGG-3′.

Statistical analysis. Data are shown as mean ± SD. In vitro experiments were performed at least in triplicate. Group comparisons were performed using two-way ANOVA test unless otherwise indicated.

RESULTS

***Aldh1a1* deficiency suppresses HF diet–induced fat formation in a sex- and fat depot–specific manner.** The RA role in HF diet–induced obesity was studied in male and female mice deficient in *Aldh1a1*, a predominant RA-generating enzyme in white adipose (15). WT and *Aldh1a1*$^{-/-}$ mice received an RC or HF diet for 180 and 300 days to explore long-term effects of HF consumption (Fig. 1). WT and *Aldh1a1*$^{-/-}$ females weighed less than male mice on an RC diet (Fig. 1*A*, day 0). On an HF diet (Fig. 1*A*, days 180 and 300), WT females and males gained weight, and sex-specific differences in weight were only modestly different after 180 and 300 days on an HF diet, respectively. *Aldh1a1*$^{-/-}$ females weighed less than *Aldh1a1*$^{-/-}$ males throughout this study. However, after 300 days on an HF diet, both male and female *Aldh1a1*$^{-/-}$ mice had significantly reduced weight compared with WT groups.

Fat accumulation on an HF diet occurred in a depot- and sex-specific manner. Subcutaneous fat accumulated to a similar extent in WT males and females (Fig. 1*B*) and was reduced to a similar extent in *Aldh1a1*$^{-/-}$ males and females. Strikingly, VF accumulation was markedly increased in WT females compared with males on an HF diet (Fig. 1*C*). In contrast, VF mass in *Aldh1a1*$^{-/-}$ females was suppressed (4.2-fold lower than in WT females), whereas VF in *Aldh1a1*$^{-/-}$ males was identical to that seen in WT males after 180 days on an HF diet (Fig. 1*C*). Longer

***F*: GTT in WT (dashed line, males [blue Xs, $n = 6$] and females [red circles, $n = 7$]) and *Aldh1a1*$^{-/-}$ (solid line, males [$n = 9$] and females [$n = 8$]). *G*: Insulin was measured in plasma of fasted mice on an HF diet by ELISA (WT, $n = 5$; KO, $n = 4$/sex-group). *H*: Food consumption was measured in WT (white bars) and *Aldh1a1*$^{-/-}$ (black bars) mice in metabolic cages ($n = 5$ in all groups). The values among groups were not statistically different. *I*: NEFA were measured in same plasma as insulin (*G*). Sub, subcutaneous fat; Vis, VF. Throughout figure legends, data are shown as mean ± SD, and statistical differences were examined by two-way ANOVA unless otherwise indicated. (A high-quality digital representation of this figure is available in the online issue.)**

durations of HF feeding (300 days) decreased VF mass in *Aldh1a1*$^{-/-}$ females (12.3-fold lower than WT females). Triglyceride (TG) content in VF of *Aldh1a1*$^{-/-}$ males underwent significant reduction (2.3-fold) compared with WT males after 300 days on an HF diet in VF (Fig. 1*C* and Supplementary Fig. 1*A*). The NEFA content in VF was not significantly different among all groups (Supplementary Fig. 1*B*). Whereas metabolic rate and respiratory quotient (RQ) were similar in WT males and females (Fig. 1*D* and *E*), *Aldh1a1*$^{-/-}$ females had a higher metabolic rate and lower RQ compared with *Aldh1a1*$^{-/-}$ males, which reached significance at some time points. Brown fat mass was similar in WT and *Aldh1a1*$^{-/-}$ females and lower in WT than in *Aldh1a1*$^{-/-}$ males (Supplementary Fig. 1*C*). Both *Aldh1a1*$^{-/-}$ males and females had improved glucose tolerance compared with respective WT groups (Fig. 1*F*); insulin levels in fasted mice were not significantly different among groups (Fig. 1*G*). Food intake monitored for 24 h in metabolic cages was comparable among all groups (Fig. 1*H*). Plasma TG levels were also similar among groups (Supplementary Fig. 1*D*). In contrast, NEFA plasma levels were higher in WT versus *Aldh1a1*$^{-/-}$ females and showed sexual dimorphism in *Aldh1a1*$^{-/-}$ mice. Therefore, *Aldh1a1* may regulate sexual divergence in metabolic responses (e.g., VF in females).

To identify retinoid-sensitive effector proteins responsible for VF reduction in *Aldh1a1*$^{-/-}$ females, we performed a comparative proteomic analysis of VF in *1*) WT versus *Aldh1a1*$^{-/-}$ males (Fig. 2*A*, *left panel*), and *2*) WT versus *Aldh1a1*$^{-/-}$ females (Fig. 2*A*, *right panel*).

Atgl is a Rald-sensitive protein contributing to visceral obesity resistance in *Aldh1a1*$^{-/-}$ females. Proteomic analysis of WT versus *Aldh1a1*$^{-/-}$ VF revealed that 176 proteins in group 1 (male) and 167 proteins in group 2 (female) differed. Among them, 13 proteins varied significantly in abundance in VF after false discovery rate correction (Fig. 2*A* and Table 1). Based on statistical significance, proteins were subdivided into groups different in *1*) females, *2*) males, and *3*) both males and females. Among proteins differentially expressed in females was a key Atgl, a PPARγ-regulated gene (31,32), which is increased in mouse VF following HF feeding (33). We analyzed mRNA and protein expression of Atgl in VF from each group (Fig. 2*B* and *C*). *Atgl* mRNA expression was similar in all mice. SVF contributed to a minor extent to Atgl mRNA and protein expression (Fig. 2*B*, inset), in consonance with previous reports (34). In contrast, Atgl protein levels and NEFA release were increased in VF of *Aldh1a1*$^{-/-}$ females compared with males (Fig. 2*C* and *D*). Correspondently, adipocyte size was also smaller in VF of *Aldh1a1*$^{-/-}$ females compared with other groups (Fig. 2*E*). Immunohistological staining (Fig. 2*F*) revealed multiple Atgl-positive multilocular clusters only in VF of *Aldh1a1*$^{-/-}$ females, in agreement with the expected lipolytic Atgl function. Recently (35–37), the function of Atgl was coupled to thermogenesis in brown multilocular fat. We and others found higher expression of thermogenic genes in the *Aldh1a1*$^{-/-}$ adipocytes and VF (21,38). The immunohistological staining of same VF sections revealed Ucp1 expression in multilocular Atgl-positive adipocytes only in *Aldh1a1*$^{-/-}$ females, whereas VF in other mice had rare interspersed Ucp1-positive adipocytes. The Ucp1 mRNA expression was 9.6-fold higher in *Aldh1a1*$^{-/-}$ females than WT males, whereas the values in male groups were not different between genotypes (Supplementary Table 1 including other relevant genes). Thus, VF underwent more profound remodeling in *Aldh1a1*$^{-/-}$ females than males.

To examine whether the sex-specific Atgl expression was dependent on Aldh1 products, we investigated the effects of Rald and RA in VF of *Aldh1a1*$^{-/-}$ male mice ex-vivo (Fig. 3*A*). Short-term stimulation (2 h) of male VF explants by Rald, but not RA, resulted in significantly increased Atgl protein levels. The estrogen effect on Atgl was examined in VF of ovariectomized WT females (Fig. 3*B* and *C*) with reduced estrogen levels (Fig. 3*B*, inset). Estrogen deficiency in ovariectomized WT females moderately increased Atgl protein levels compared with sham-operated animals, but this trend did not reach statistical significance (Fig. 3*B*). *Atgl* mRNA expression was identical in both groups (Fig. 3*C*). Given the minor effects of estrogen on Atgl protein levels, we examined the effect of retinoids on the regulation of this protein. Short-term stimulation with Rald increased Atgl protein levels in mature 3T3-L1 adipocytes (Fig. 3*D*). Stimulations with retinol or RA did not influence Atgl protein levels. The potential dependence of Rald's effects on Atgl translation was examined in the presence of cycloheximide, an inhibitor of protein biosynthesis (Fig. 3*E*). Long-term (30 h) pretreatment with cycloheximide prevented Rald-mediated induction of Atgl protein, seen at short (6 h) pretreatment of 3T3-L1 adipocytes, suggesting mechanisms dependent on protein biosynthesis. Next, we examined sexual dimorphisms in *Aldh1* enzymes responsible for Rald catabolism.

Expression of *Aldh1* enzymes is sex-specific in VF. Aldh1 enzymes were expressed in a sex-specific fashion that was particularly apparent in *Aldh1a1*$^{-/-}$ mice (Fig. 4*A*). *Aldh1a1*, the major RA-producing enzyme in adipocytes (15), was expressed at markedly higher levels than *Aldh1a2* and *Aldh1a3* in VF of WT male and female mice. In SVF isolated from VF, Aldh1a1 expression was low and comparable with Aldh1a2 and -a3 expression levels (Fig. 4*A*, inset). The expression of *Aldh1a2* and *Aldh1a3* was sex-specific and lower in WT females than in WT males. In the genetic absence of *Aldh1a1*, expression of *Aldh1a2* and *Aldh1a3* was lower in *Aldh1a1*$^{-/-}$ females than males. Expression of *Cyp26A1*, an RA-sensitive gene (39), was also significantly lower in *Aldh1a1*$^{-/-}$ female, but not male, mice compared with their respective WT groups (Fig. 4*B*). To investigate whether inhibition of *Aldh1a2* and/or *Aldh1a3* was mediated by estrogen, we measured the expression of these enzymes in ovariectomized mice (Fig. 4*C*). Only *Aldh1a3* expression was significantly increased (180%) in ovariectomized compared with sham-operated WT females. Interestingly, *Aldh1a3* expression was 188% higher in male compared with female WT mice on a regular diet without surgical intervention (Fig. 4*C*, inset). In consonance with the role of Aldh1a3 in RA generation, *Cyp26A1* expression also was higher in this animal group (Fig. 4*D*). Ovariectomized WT mice gained weight and VF compared with sham-operated WT mice (120 and 217%, respectively) (Fig. 4*E* and *F*). VF in ovariectomized *Aldh1a1*$^{-/-}$ females underwent a moderate (167%) but not significant increase in VF compared with the sham-operated *Aldh1a1*$^{-/-}$ group and reached levels seen in WT sham-operated mice (Fig. 4*F*). Ovariectomy in *Aldh1a1*$^{-/-}$ females also moderately increased *Aldh1a2* and *-a3* expression (Fig. 4*F*, inset). Correspondent to VF changes, ovariectomized groups had impaired glucose tolerance; however, *Aldh1a1*$^{-/-}$ females were more glucose tolerant than WT in both sham and ovariectomized groups (Fig. 4*G*). Postprandial plasma

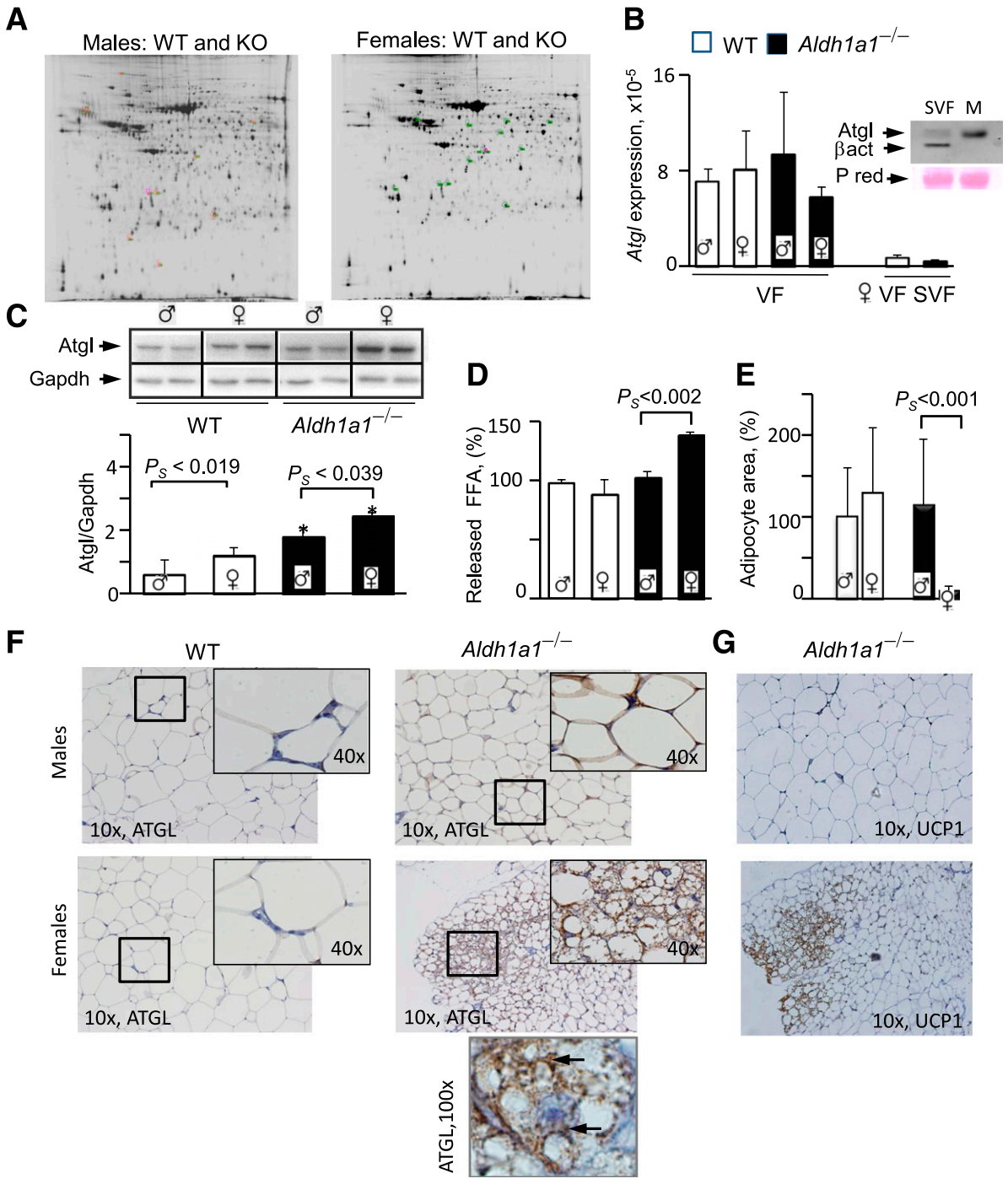

FIG. 2. Sex-specific proteome and Atgl protein levels in VF of WT and *Aldh1a1*$^{-/-}$ mice. *A*: Representative images of the DIGE proteomic gels comparing cy2-, cy3-, and cy5-stained proteins from VF isolated from WT and *Aldh1a1*$^{-/-}$ males (180-day HF groups). Four gels from four pairs of different WT and *Aldh1a1*$^{-/-}$ VF pads were run in each experiment. Spots, 176 in male (*left panel*) and 167 in female (*right panel*) groups, were different between WT and *Aldh1a1*$^{-/-}$ mice without false discovery rate correction (FDRC) and 13 proteins after FDRC analysis. The identified 13 spots are shown on the gel image as a square around a spot that was significantly changed by at least 1.5-fold between groups with $P \leq 0.05$ after FDRC using an independent *t* test. *Atgl* mRNA expression levels were measured by TaqMan (*B*, VF group), and Atgl protein levels (*C*) were analyzed by Western blot in VF from WT and *Aldh1a1*$^{-/-}$ male and female mice (all mean ± SD; $n = 4$) on an HF diet as well as in SVF fraction isolated from three age-matched females on a regular diet (*B*, SVF VF group for mRNA expression). Inset in *B* confirms negligible Atgl protein levels in SVF compared with mature (M) adipocytes from same WT female using Western blot. Inset in *C* shows Atgl protein levels in two animals from each group. gapdh, glyceraldehyde-3-phosphate dehydrogenase. *Significant difference between WT vs. KO groups. *D*: Release of NEFA from VF explants (0.1 g WT males and females, 0.08 g knockout [KO] males, and 0.06 g KO females using 5 mL medium/g fat) stimulated with isoproterenol for 1.5 h in DMEM containing 2% delipidated BSA. VF was isolated from three mice per group. Data were normalized to the levels seen in WT male mice (100%). FFA, free fatty acid. *E*: Area of unilocular adipocytes was quantified from the images (original magnification ×10) shown in *F*. Total of 300 adipocytes were quantified per group. *F*: Representative Atgl staining of paraffin-embedded VF from WT and *Aldh1a1*$^{-/-}$ male and female mice (all $n = 4$; mean ± SD) on an HF diet (180 days). In *Aldh1a1*$^{-/-}$ female mice, Atgl protein was found in multilocular adipocytes. 10×, 40×, and 100× indicates magnification. Arrows in ×100 original magnification group show cytosolic and perilipid droplet Atgl staining in a multilocular adipocyte. *G*: Representative Ucp1 staining of same sections from *Aldh1a1*$^{-/-}$ male and female mice. Brown Ucp1 staining was associated with multilocular adipocytes. P_S, significantly different between male and female *Aldh1a1*$^{-/-}$ mice. (A high-quality digital representation of this figure is available in the online issue.)

TABLE 1
Proteins identified in proteomic analysis for which protein levels were altered in VF from *1*) WT and *Aldh1a1*$^{-/-}$ male groups; *2*) WT and *Aldh1a1*$^{-/-}$ female groups; or *3*) both differences in protein levels of proteomic markers measured in the two following groups: *1*) male WT and *Aldh1a1*$^{-/-}$ mice and *2*) female WT and *Aldh1a1*$^{-/-}$ mice, using proteomic DIGE analysis

Protein name	Average ratio males	*P* value males	Average ratio females	*P* value females	Verification
Females					
Bckdh	1.54	NS	2.03	0.038	QPCR
Atgl	2.03	NS	1.57	0.05	W, QPCR
Plastin-2	−3.3	NS	−2.8	0.05	QPCR
Carnosinase-2	−1.94	NS	−1.72	0.05	QPCR
Cmbp-5	−1.5	NS	−1.58	0.013	QPCR
Caspase-1	−1.14	NS	−1.54	0.000	QPCR
Males					
Glia maturation factor β	9.85	0.008	8.01	NS	W, QPCR
Serine protease inhibitor A3K	5.43	0.047	2.12	NS	QPCR
Triacylglycerol hydrolase	2.23	0.021	2.43	NS	QPCR
Nidogen-1 precursor	1.57	0.037	−1.04	NS	QPCR
Both groups					
Peroxiredoxin-6	9.47	0.008	6.28	0.002	W, QPCR
Glod4	5.26	0.003	5.26	0.008	QPCR
Bpnt1	2.56	0.037	2.82	0.005	QPCR

Average ratio represents fold change (+, increase; −, decrease) of this protein compared with standardized control containing all samples; *t* test ($n = 4$). TaqMan (quantitative PCR [QPCR]) or Western blot (W) analyses that were performed to verify these findings are denoted in the last column. Bckdh, 2-oxoisovalerate dehydrogenase subunit b; Bpnt1, 3′(2′),5′-bisphosphate nucleotidase 1; Cmbp-5, charged multivesicular body protein 5; Glod4, glyoxalase domain-containing protein 4.

insulin levels were similar in all groups. Thus, sex specificity in Rald catabolism may depend on estrogen, which reduced *Aldh1a3* expression in female mice, decreased VF formation, and improved glucose metabolism.

Although the *Aldh1a1*$^{-/-}$ model established causal relationships between Aldh1 enzymes and obesity, it does not provide insight into intrinsic RARE activation in relation to RA-generating Aldh1 enzymes in vivo, which is heavily influenced by sex hormone production and diet. For example, ultradian estrogen production and feeding-starvation cycles may alter RA production and RAR activation in a spatiotemporal fashion in adipocytes, which cannot be well-characterized in the previously used animal models. In order to better examine RAR regulation in subcutaneous and visceral adipose over time, a RARE-lacZ reporter mouse model was used.

Sex- and depot-specific RA formation accompanies HF diet–induced obesity in RARE-LacZ mice. The RARE-lacZ reporter model was developed and is widely used to monitor progressive spatiotemporal changes in auto- and paracrine RAR activation during embryogenesis in *Aldh1*-deficient mouse models (28,40,41), reviewed by Duester (14). In this model, activated RARs (e.g., due to increased intracellular RA concentrations) bind to native and transgenic RARE coupled to β-galactosidase expression. Thus, β-galactosidase expression in these mice provides cumulative information about RAR regulation. We verified that adult RARE-lacZ mice responded to nanomolar RA concentrations in circulation (Supplementary Fig. 2*A* and *B*). Intraperitoneal RA administration increased β-galactosidase protein expression in liver and adipose tissue in RARE-lacZ but not in WT mice. Accordingly, only RARE-lacZ mice expressed β-galactosidase mRNA in the liver (Supplementary Fig. 2*C*). Stimulation of VF explants from RARE-lacZ males with RA increased β-galactosidase expression (Fig. 5*A*), whereas Rald did not influence β-galactosidase expression, in agreement with the low binding affinity of this metabolite to RAR (22). The natural RARE-containing target genes *Cyp26A1* and *Cyp26B1* were also regulated by RA, but not by Rald (Fig. 5*B* and *C*).

RARE-lacZ male and female mice gained weight on an HF compared with a regular diet (data not shown) due to increased subcutaneous and VF mass (Fig. 5*D* and *E*). Formation of subcutaneous fat was increased at comparable levels in male (261%) and female (221%) RARE-lacZ mice on an HF compared with a regular diet (Fig. 5*D*). HF diet consumption resulted in a significant increase in VF formation in both groups (Fig. 5*E*) and an increased ratio of visceral to subcutaneous fat in females (1.6 in males vs. 2.6 in females) (Fig. 5*E*, inset).

β-Galactosidase expression, a surrogate measure of RARE activation, was similar in subcutaneous fat of males and females on RC, whereas in VF, males expressed significantly more β-galactosidase than females (Fig. 5*F*). On the HF compared with regular diet, subcutaneous fat formation was accompanied by increased β-galactosidase expression in both male (363%) and female (495%) RARE-lacZ mice (Fig. 5*G*). Strikingly, VF formation in RARE-lacZ males was not associated with β-galactosidase expression, whereas in RARE-lacZ females, VF formation was accompanied by an 860% increase in β-galactosidase expression in HF versus regular diet groups. These experiments suggest that an HF diet induces RARE in VF, and retinoid production may underlie sex-specific effects.

Obese men and women express higher levels of *Aldh1* enzymes in SVF than lean subjects. In a pilot investigation, we examined omental adipose from lean and obese patients (Table 2). *Aldh1* expression in the whole VF was not different in obese and lean patients. We then examined *Aldh1* expression in the SVF. *Aldh1a1* was the most abundantly expressed isoform in the SVF and was expressed at significantly higher levels in obese than in lean women (333%) (Fig. 6*A*). *Aldh1a3* expression was higher in obese (422%) than in lean men. Thus, increases in the major Aldh1 isoform may preferentially drive RA production and its obesity responses in females more than in males. Next, we examined whether retinoids or E2 also

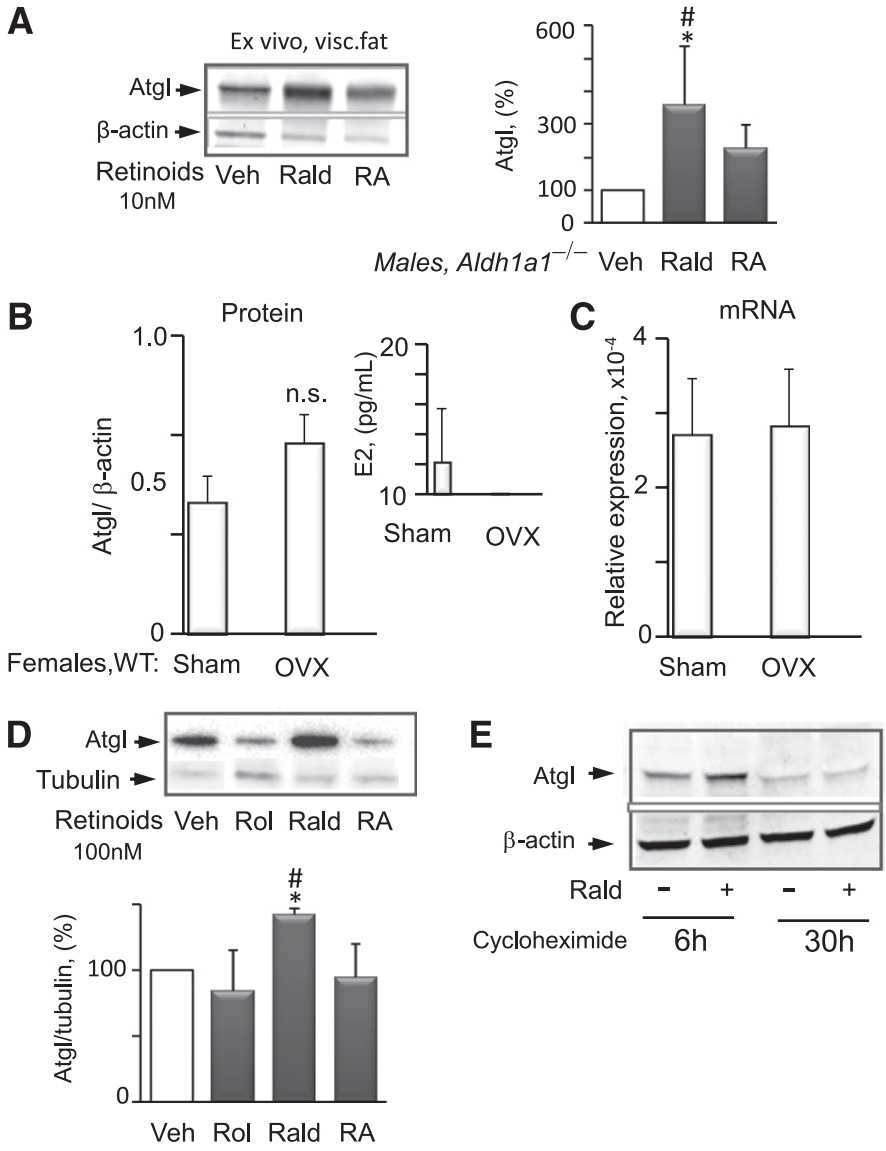

FIG. 3. Rald regulates Atgl protein levels in *Aldh1a1*$^{-/-}$ male VF ex vivo and in differentiated 3T3-L1 adipocytes in vitro. *A*: Atgl protein levels in VF explants isolated from *Aldh1a1*$^{-/-}$ males (n = 3) were measured by Western blot. Three VF pads dissected from each animal (equal by weight 76 mg) were immediately stimulated with vehicle, RA, and Rald (all 10 nmol/L) for 2 h. Atgl levels were normalized to housekeeping proteins β-actin or glyceraldehyde-3-phosphate dehydrogenase. Data for each set (inset) were normalized to vehicle control (100%) for VF from each animal. *Difference between control (Veh) and Rald-explants (P < 0.05) (all mean ± SE; n = 3); #difference between Rald- and RA-stimulated explants (P < 0.05). Visc, visceral. *B*: Atgl protein levels were analyzed by Western blot in VF from C57BL/6J (WT) ovariectomized and sham-operated female mice (all mean ± SE; n = 4). Inset shows estrogen (E2) levels in plasma using ELISA. *C*: *Atgl* mRNA expression levels were measured by TaqMan in the same VF. Mann-Whitney *U* test analysis showed no significance between groups. *D*: Atgl levels in differentiated (8 days) 3T3-L1 fibroblasts measured by Western blot. Cells were stimulated for 45 min with retinol (Rol), RA, and Rald (all retinoids 100 nmol/L) in 100 nmol/L insulin/20% FBS medium. Atgl levels were normalized to tubulin. Data are shown as a percent of vehicle control. Inset at *top* shows a representative example of a Western blot. *Difference between control (Veh) and Rald-stimulated cells; #difference between Rald- and RA-stimulated cells, both P < 0.05 (mean ± SE; n = 3). *E*: Atgl levels in differentiated (8 days) 3T3-L1 fibroblasts stimulated with cycloheximide (20 μg/mL) for 6 or 30 h. The cycloheximide-treated adipocytes were stimulated with vehicle and Rald (10 nmol/L) for an additional 45 min. Atgl and β-actin levels were measured by Western blot. Prolonged (30 h) cycloheximide treatment inhibited protein translation and abolished the Rald-dependent increase in Atgl protein levels.

influence NEFA release in differentiated human SGBS adipocytes (Fig. 6*B*). Stimulation of SGBS with Rald, but not RA, increased NEFA release, in agreement with the response seen in mouse VF explants (Fig. 2*D*), supporting a possible role of retinoids regulated by Aldh1 in adipocytes.

DISCUSSION

HF diet and hormonal changes associated with menopause are well known to alter adipose distribution in women (9) and C57BL/6J female mice (42) from a predominantly subcutaneous pattern to excess visceral deposition. The mechanisms for this redistribution are hitherto not described. In this study, we show that HF feeding induces autocrine RA formation that, in turn, governs fat formation in a depot- and sex-specific fashion. Our data suggest that an HF diet and/or lack of estrogen mediates VF formation through a sex-specific autocrine *Aldh1* switch, in which lipolysis, mediated by an induction of Atgl through Rald, is replaced by RA-mediated lipid accumulation. These results in mice were paralleled by increased expression of *Aldh1a1* in obese women.

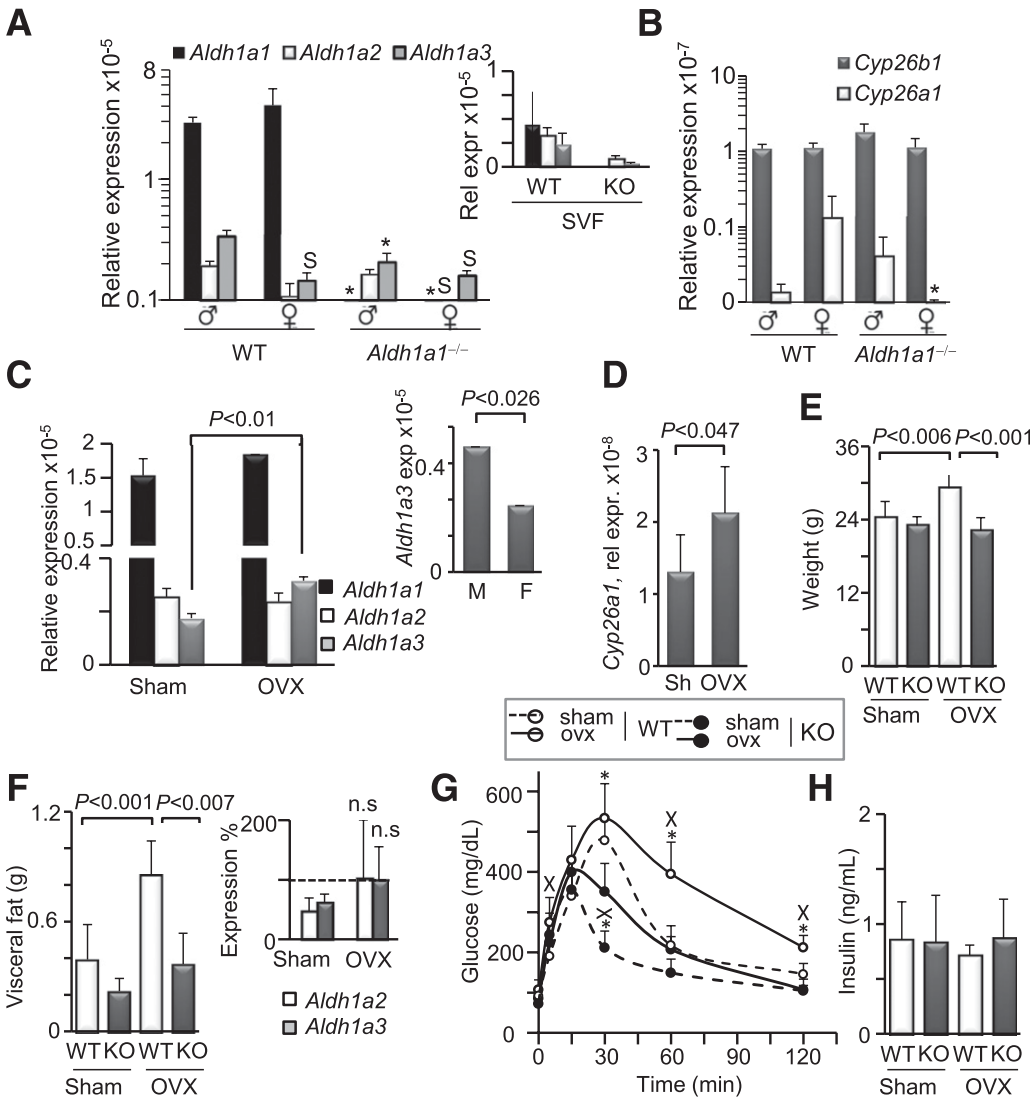

FIG. 4. Estrogen contributes to sex-specific expression of *Aldh1* enzymes in VF. Relative expression (Rel expr) of RA-generating *Aldh1* enzymes (*A*) and RARE containing RA target genes *Cyp26A1* and *Cyp26B1* (*B*) in VF isolated from WT male (n = 5), female (n = 4), and *Aldh1a1*$^{-/-}$ male and female mice (both n = 4) on an HF diet (180 days). All data are shown as mean ± SE. *P < 0.001 differences between genotypes in the same sex-group; SP < 0.05, significant differences between sexes within one genotype. Inset in *A* shows *Aldh1* expression in SVF fraction in age-matched females on RC (same n = 3/group as in Fig. 2*B*). Relative expression of *Aldh1* enzymes (*C*) and *Cyp26A1* (*D*) enzymes was measured in VF isolated from sham-operated (Sh; n = 5) and ovariectomized (OVX; n = 4) WT female mice (same study as Fig. 3*B*). Inset shows *Aldh1* expression (exp) in WT male (M; n = 4) and female (F; n = 5) group on a regular diet (same as in Fig. 1, 0 time). Data are shown as mean ± SD. P value was determined by Mann-Whitney U test. Weight (*E*) and VF mass (*F*) in sham-operated and ovariectomized WT (Sham, n = 10; OVX, n = 8) and *Aldh1a1*$^{-/-}$ (Sham, n = 9; OVX, n = 5) mice. Inset shows expression levels of Aldh1a2 and -a3 enzymes in sham and OVX *Aldh1a1*$^{-/-}$ mice (n = 5/group). Data are shown as percentage of values seen in WT sham-operated mice (dashed line). *G*: GTT in WT (open circles; sham, dashed and ovx, solid lines) and *Aldh1a1*$^{-/-}$ (closed circles; sham, dashed and ovx, solid lines) mice (n = 4 in WT sham and n = 5 in all other groups). *P < 0.001 differences between genotypes in sham or OVX group; Xdifferences (P < 0.04 or less) between sham and OVX mice within one genotype. *H*: Insulin levels were measured by ELISA in plasma isolated from sham-operated and OVX WT and *Aldh1a1*$^{-/-}$ mice (n = 4/group). Insulin levels were not significantly different (Mann-Whitney U test). n.s., not significantly different by two-way ANOVA.

Our previous studies demonstrated that Aldh1a1 is the major RA-generating enzyme in mice (15). In this study, we showed that disruption of RA production by Aldh1a1 impaired VF formation in females more than in males. *Aldh1a1* deficiency in females prevented development of HF diet–induced visceral obesity in WT mice. In males, HF diet modestly impaired VF formation that was significantly reduced in *Aldh1a1*$^{-/-}$ males only after being on an HF diet for a prolonged (>180 days) period of time. Notably, WT male and female mice had equal increases in the formation of subcutaneous fat on an HF diet that were reduced to comparable levels in *Aldh1a1*$^{-/-}$ males and females.

Comparison of the proteomic analysis of VF in WT and *Aldh1a1*$^{-/-}$ male and female groups enabled the identification of candidate proteins that could explain divergent lipid metabolism and VF formation in *Aldh1a1*$^{-/-}$ males and females. We scrutinized the regulation of Atgl (among 13 others), considering its central role in TG hydrolysis and adipose homeostasis (32). Increased TG lipolysis is required to support thermogenic function through a PPARα-mediated mechanism (36,37). Thermogenesis in both white and brown fat was elevated in *Aldh1a1*$^{-/-}$ mice as shown previously (20,21,38). Consistent with a potential role, Atgl protein levels and NEFA release were markedly higher in *Aldh1a1*$^{-/-}$ females than in males. In vivo,

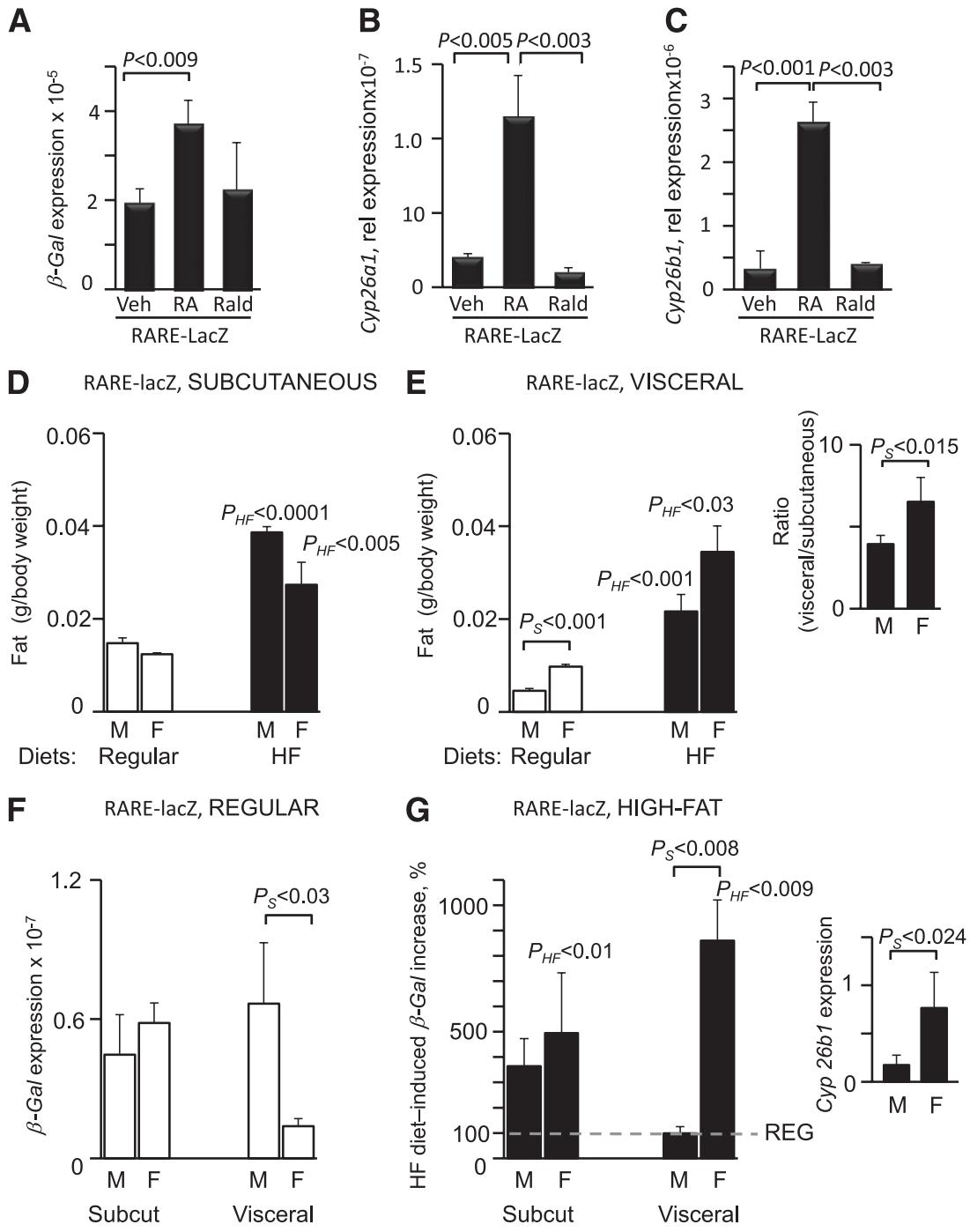

FIG. 5. Depot- and sex-specific RARE activation accompanies HF diet–induced fat formation in RARE-lacZ mice. *A*: mRNA β-galactosidase (β-Gal) expression in VF explants from RARE-lacZ male mice treated with RA and Rald (both 10 nmol/L) for 3 h in 1% UV-treated FBS in DMEM. Immediately after excision, explants were transferred to 1% UV-treated FBS in DMEM for 12 h prior to stimulation with RA. *P* value indicates significant induction by RA, but not Rald. mRNA *Cyp25a1* (*B*) and *Cyp26b1* (*C*) expression in VF explants from RARE-lacZ male mice treated with RA and Rald (both 10 nmol/L) for 12 h in 1% UV-treated FBS in DMEM. These RAR target genes are under control of a natural RARE promoter and required longer incubation time for expression upon induction by retinoids. Relative weight (fat pad mass per body mass) of subcutaneous (Subcut; inguinal) (*D*) and visceral (perigonadal) (*E*) fat in male (M) and female (F) RARE-lacZ mice receiving regular (white bars) and HF diets for 5 months. Data are shown as mean ± SE; $n = 5$ in each of the four groups. P_{HF} indicates significant differences between mice (same sex group) receiving a regular or HF diet; P_S indicates significant differences between males and females receiving similar chow diets. Inset in *E* shows the significantly higher ratio of VF to subcutaneous fat in RARE-lacZ female compared with male mice on an HF diet. *F*: Relative β-Gal expression in subcutaneous and VF isolated from RARE-lacZ males and females on an RC diet. β-Gal expression was normalized to 18S expression by threshold cycle method. P_S indicates significantly higher β-Gal expression in male compared with female VF. *G*: Increase in β-Gal expression (%) in visceral adipose depots in RARE-lacZ mice receiving HF compared with regular diet (100%, dashed gray line). P_{HF} indicates significant differences between mice (same sex-group) receiving regular (shown in *C*) or HF diet. P_S shows significant induction of β-Gal expression (%) in female compared with male VF.

TABLE 2
Biomorphic data of human subjects

	Lean females	Lean males	Obese females	Obese males
Age (years)	48.7 ± 8.0	59.9 ± 5.6	46.1 ± 5.1	38.4 ± 2.7
Height (inches)	65.5 ± 1.5	69.7 ± 1.1	63.3 ± 1.2	71.2 ± 1.7
Weight (pounds)	153.5 ± 4.9	171.0 ± 6.2	287.9 ± 21*#	360.3 ± 66*#
BMI	25.2 ± 0.8	24.8 ± 0.8	50.2 ± 2.1*#	49.9 ± 6.8*#
Glucose (mg/dL)	88.3 ± 7.1	89.3 ± 4.2	101.4 ± 10.3#	128.3 ± 31.8#
Insulin (μU/mL)	6.46 ± 2.2	5.3 ± 1.5	13.3 ± 4.3	13.7 ± 8.1
HOMA-IR	1.36 ± 0.4	1.2 ± 0.4	3.6 ± 1.5	3.4 ± 1.0
QUICKI	0.38 ± 0.03	0.39 ± 0.02	0.34 ± 0.02	0.32 ± 0.01
HbA_{1c} (%)	5.63 ± 0.20	5.45 ± 0.10	5.93 ± 0.25	6.4 ± 1.0
TG (mg/dL)	92.5 ± 14.6	137.3 ± 45	101.6 ± 16	183.7 ± 83
CRP (mg/dL)	3.83 ± 3.2	1.54 ± 0.90	11.6 ± 3.3#	11.9 ± 8.0#
TC (mg/dL)	174.8 ± 16.8	191.3 ± 21	167 ± 19	156.3 ± 7.8
HDL (mg/dL)	46.3 ± 1.1	52.5 ± 6.1	43.6 ± 3.6#	27.3 ± 3.9*#
LDL (mg/dL)	109.8 ± 19	111.3 ± 22	103.0 ± 16	92.3 ± 10
TZD	0	0	2	0

Differences in biomorphic data and serum levels of lipoproteins and inflammatory markers in lean and obese men and women. Serum markers of glucose/insulin control (fasting glucose, insulin, HbA_{1c}), C-reactive protein (CRP), and a lipid panel were measured at The Ohio State University Medical Center. The homeostatic model assessment-insulin resistance (HOMA-IR) was calculated using the formula (Go × Io)/22.5, where Go is fasting glucose and Io is fasting insulin. Quantitative Insulin Sensitivity Check Index (QUICKI) was calculated using the formula 1/(log[Io] + log[Go]). TC, total cholesterol; TZD, thiazolidinedione. *$P < 0.05$ versus same sex control. #$P < 0.05$, lean both sexes vs. obese both sexes. Statistical analysis was performed using two-way ANOVA with Bonferroni posttest.

adipocytes were smaller, multilocular, and expressed Atgl and Ucp1 protein in VF in *Aldh1a1*$^{-/-}$ females, but not in males. These increased Atgl levels in numerous thermogenic visceral adipocytes (36,37) along with increased metabolic rate may provide a potential explanation for the ability of *Aldh1a1*$^{-/-}$ females to resist pronounced visceral obesity seen in WT females in response to an HF diet. In consonance with this interpretation, the implantation of thermogenic *Aldh1a1*$^{-/-}$ preadipocytes into VF of WT mice limited VF development on an HF diet compared with mice treated with WT preadipocytes (38).

To further delineate the role of Rald and estrogen in sex-specific responses, we studied the effects of these two mediators on Atgl. In the absence of estrogen, ovariectomized WT females had increased expression of *Aldh1a3* and *RAR* target genes (*Cyp26A*), suggestive of RA generation. These experiments highlight an indirect participatory role of estrogen in Atgl regulation, perhaps via its inhibition of *Aldh1* expression. Estrogen regulation of Aldh1 enzymes has been previously reported in other tissues (23). In both obese mice and obese women, *Aldh1a1* overrides expression of *Aldh1a2* and *-a3* enzymes (Figs. 4 and 6). Consequently, Rald catabolism was markedly impaired in *Aldh1a1*$^{-/-}$ females, whereas *Aldh1a1*$^{-/-}$ male mice used Rald for RA production by the alternative Aldh1a2 and Aldh1a3 enzymes. The experiments with Rald in cultured tissue and adipocytes suggest that this metabolite can induce Atgl protein but not mRNA levels in VF within hours of stimulation. A nongenomic/nontranscriptional action of Rald was confirmed using cycloheximide. Thus, Rald may exert both nongenomic and genomic effects (Fig. 6*C*), as has been described for a number of hormones, including estrogen and RA (43–45).

A unique aspect of this investigation was the assessment of cumulative RARE activation, possibly by RA production in adipose tissue in response to an HF diet over extended periods of time, when RA generation may be under the control of protean influences, including circadian/ultradian hormones and food intake. We took advantage of the RARE-lacZ reporter mice, which express β-galactosidase upon RAR activation by endogenous or added RA. By using this model in embryogenesis studies, researchers eventually mapped Aldh1 enzyme expression and identified RAR-dependent transcriptional responses in tissues and single cells (28,40,41), reviewed in Duester (14). RARE was activated in subcutaneous fat in comparable amounts in males and females, whereas VF formation was sex-specific. On a regular diet, VF in females generated substantially less RARE activity than in males. This was changed on an HF diet. Although VF was formed in both groups, only visceral obesity in females was associated with the induction of RARE. Genetic disruptions of several enzymatic pathways responsible for vitamin A metabolism led to markedly altered fat formation (15,20,46–49). The *Aldh1a1* and hormone-sensitive lipase-deficient models are characterized by impaired RA production and resistance to HF diet–induced obesity (15,49). Moreover, the administration of RA in these mice partially compensated for gene loss and improved adipogenesis in vitro and in vivo, which was consistent with RA's role in the induction of *PPARγ* expression and adipogenesis (11,15). Physiologic RARE activation, seen in RARE-lacZ mice in response to HF diets, supports RA's auto- or paracrine participation in female visceral obesity.

In additional studies of morbid obesity, we demonstrate a shift toward higher RA production in the SVF of human visceral (omental) adipose. These changes were related to higher *Aldh1* expression in obese compared with lean patients (Fig. 6*A*). Obese men demonstrated an increase in the expression of the minor isoform *Aldh1a3*. In obese women, RA generation was supported by elevated *Aldh1a1* expression, in line with possible *Aldh1a3* suppression by estrogen. In our previous studies, we showed that ectopic expression of either *Aldh1a1* or *Aldh1a3* increases intrinsic RA formation and promotes adipogenesis (15). Notably, although *Aldh1a1* induction accompanies adipogenesis, its levels remained similar in mature adipocytes (15), underscoring the role of Aldh1a1

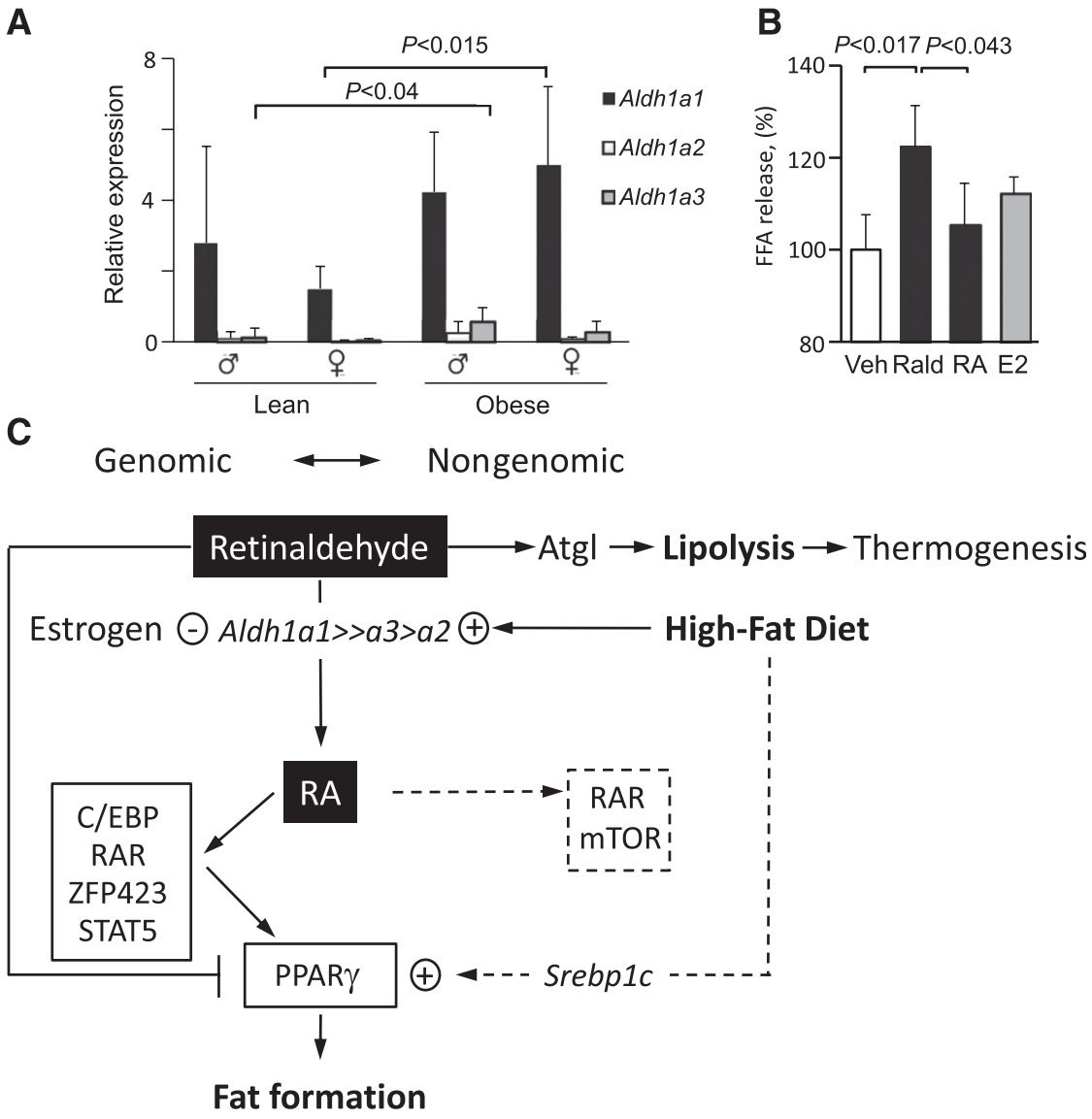

FIG. 6. Adiposity in humans is accompanied by increased *Aldh1* expression in visceral SVF cells in obese versus lean subjects and increased release of NEFA by Rald. Schematic of hypothetical Aldh1 role in sexual dimorphism in VF. *A*: *Aldh1* expression was analyzed in stromal vascular cells isolated from visceral (omentum) fat from lean (men, *n* = 6; women, *n* = 4) and morbidly obese (men, *n* = 3; women, *n* = 7) patients by TaqMan assay and normalized to hypoxanthine phosphoribosyltransferase 1. *P* indicates significance levels determined by two-way ANOVA with Bonferroni posttest. *B*: NEFA release from 13 day–differentiated human SGBS adipocytes after stimulation with vehicle (Veh), Rald (100 nmol/L), RA (100 nmol/L), and estrogen (E2; 10 nmol/L) for 3 h in medium containing 2% delipidated BSA (*n* = 3/group). For differentiation, cells were stimulated with 20 nmol/L human insulin, 0.01 mg/mL transferrin, 0.1 μmol/L cortisol, 200 pmol/L triiodothyronine, 500 μmol/L isobutylmethylxanthine (IBMX), 2 μmol/L rosiglitazone (BRL), 1% (volume for volume) biotin and pantothenic acid, and 0.25 μmol/L dexamethasone for 4 days and then for 3 days. For the remaining 7 days, cells were maintained in same media without IBMX. On day 13 of differentiation, cells were stimulated with estrogen or retinoids for 24 h. On day 14, cells were again stimulated with estrogen or retinoids in fresh medium, containing 2% delipidated BSA instead of FBS, for 3 h. *P* indicates significant changes in NEFA released from Rald-stimulated SGBS adipocytes compared with both vehicle and RA-treated group. FFA, free fatty acid. *C*: Males and females have different expression of *Aldh1* enzymes, which regulate dissimilar Rald conversion to RA. Estrogen represses *Aldh1a3* expression, whereas HF diet consumption increases *Aldh1a1* expression in women. RA has multiple genomic effects in adipose tissue and regulates expression of numerous transcription factors, culminating in the expression of *PPARγ* (reviewed in Ref. 11), adipocyte differentiation, and fat formation. RA also regulates nongenomic effects (dashed lines) through cytosolic RAR and/or mammalian target of rapamycin (mTOR) in different tissues (43,44); however, the relevance of these signaling pathways for adipose tissue has not been established. In the absence of *Aldh1a1* and reduced expression of *a2* and *a3* in females, Rald is not converted to RA and supports Atgl-mediated lipolysis in thermogenic multilocular adipocytes in VF of females, resulting in resistance to HF diet–induced fat formation in this depot. Atgl-mediated lipolysis can play a causative role in the induction of thermogenesis through the generation of PPARα ligands, which activate PPARα and its target gene Ucp1 (36,37). Rald has also been shown to suppress PPARγ and RXR activation and fat formation (20). Shown is Rald's role in the fast nongenomic regulation of Atgl protein levels, a TG-hydrolyzing protein in adipose tissue.

in preadipocytes. The increased *Aldh1*expression in SVF may indicate accelerated preadipocyte differentiation in obese versus lean patients. The changes in Rald catabolism can potentially influence NEFA hydrolysis in differentiated human adipocytes, seen in a model SGBS cell line. Aldh1 effects on lipogenesis, thermogenesis, glucose utilization, and immune and other responses in human VF remain to be investigated.

We described a mechanism by which Aldh1a1 integrates dietary and hormonal responses that could account for the regulation of susceptibility to visceral obesity in women. The identified sexual dimorphism in RA generation offers an

opportunity for further investigation of sex differences in pathways determining visceral adiposity and in devising sex-specific treatment of obesity.

ACKNOWLEDGMENTS

This research was supported by the College of Education and Human Ecology (EHE) Seed Grant, Food Innovation Center Seed Grant, The Ohio State University (OSU) International Office Seed Grant, and a Pilot Industry Partnership grant to the OSU Center for Clinical and Translational Science, which was supported by Award UL1RR025755 from the National Center for Research Resources (to O.Z.), National Institutes of Health (NIH) grants R01-ES-017290 and R21-DK-088522 (to S.R.), Alpha Omega Alpha Honor Medical Society 2011 Carolyn L. Kuckein Student Research Fellowship (to B.R.), grants R01-EY-013969 (to G.D.) and P30-CA-16058-30 (to K.B.G.), an NIH National Cancer Institute OSU Comprehensive Cancer Center Support Grant (to K.B.G.), and a National Research Service Award grant (F32-DK-083903 to J.D.). This research was also supported by an EHE Dissertation fellowship from the College of Education and Human Ecology (to R.Y.). The funders had no role in study design, data collection and analysis, decision to publish, or preparation of the manuscript.

No potential conflicts of interest relevant to this article were reported.

R.Y. researched RARE data, provided evidence of non-genomic Rald function, and contributed to discussion. B.R. developed the ovariectomy procedure, researched Atgl data, and edited the manuscript. J.D. researched human data and edited the manuscript. F.Y. developed the ovariectomy procedure. A.L. and J.M. researched RARE data. M.S. collected tissue samples for 180d and edited the manuscript. S.S. conducted SVF isolation in mice. K.S.V. collected tissue samples for 180d. K.B.G. supervised proteomic analysis. K.L. contributed to the primary adipocyte studies, contributed to discussion, and edited the manuscript. H.A. supervised TaqMan analysis. G.D. created knockout mice and reviewed the manuscript. R.Z. supervised ATGL studies in SGBS adipocytes. S.R. supervised human studies and reviewed the manuscript. O.Z. designed and supervised experiments and wrote the manuscript. All authors reviewed and edited the manuscript. O.Z. is the guarantor of this work and, as such, had full access to all the data in the study and takes responsibility for the integrity of the data and the accuracy of the data analysis.

The authors thank M. Kleinholz and R. Sessler (Mass Spectrometry and Proteomic Facility, The Ohio State University) for excellent technical support.

REFERENCES

1. Li C, Ford ES, McGuire LC, Mokdad AH. Increasing trends in waist circumference and abdominal obesity among US adults. Obesity (Silver Spring) 2007;15:216–224
2. Empana JP, Ducimetiere P, Charles MA, Jouven X. Sagittal abdominal diameter and risk of sudden death in asymptomatic middle-aged men: the Paris Prospective Study I. Circulation 2004;110:2781–2785
3. Canoy D, Boekholdt SM, Wareham N, et al. Body fat distribution and risk of coronary heart disease in men and women in the European Prospective Investigation Into Cancer and Nutrition in Norfolk cohort: a population-based prospective study. Circulation 2007;116:2933–2943
4. Zhang C, Rexrode KM, van Dam RM, Li TY, Hu FB. Abdominal obesity and the risk of all-cause, cardiovascular, and cancer mortality: sixteen years of follow-up in US women. Circulation 2008;117:1658–1667
5. Deshmukh-Taskar PR, O'Neil CE, Nicklas TA, et al. Dietary patterns associated with metabolic syndrome, sociodemographic and lifestyle factors in young adults: the Bogalusa Heart Study. Public Health Nutr 2009;12:2493–2503
6. Koutsari C, Ali AH, Mundi MS, Jensen MD. Storage of circulating free fatty acid in adipose tissue of postabsorptive humans: quantitative measures and implications for body fat distribution. Diabetes 2011;60:2032–2040
7. Zamboni M, Armellini F, Milani MP, et al. Body fat distribution in pre- and post-menopausal women: metabolic and anthropometric variables and their inter-relationships. Int J Obes Relat Metab Disord 1992;16:495–504
8. Tchoukalova YD, Koutsari C, Votruba SB, et al. Sex- and depot-dependent differences in adipogenesis in normal-weight humans. Obesity (Silver Spring) 2010;18:1875–1880
9. Perrini S, Leonardini A, Laviola L, Giorgino F. Biological specificity of visceral adipose tissue and therapeutic intervention. Arch Physiol Biochem 2008;114:277–286
10. Pasquali R. Obesity and androgens: facts and perspectives. Fertil Steril 2006;85:1319–1340
11. Yasmeen R, Jeyakumar SM, Reichert B, Yang F, Ziouzenkova O. The contribution of vitamin A to autocrine regulation of fat depots. Biochim Biophys Acta 2012;1821:190–197
12. Germain P, Chambon P, Eichele G, et al. International Union of Pharmacology. LX. Retinoic acid receptors. Pharmacol Rev 2006;58:712–725
13. Germain P, Chambon P, Eichele G, et al. International Union of Pharmacology. LXIII. Retinoid X receptors. Pharmacol Rev 2006;58:760–772
14. Duester G. Retinoic acid synthesis and signaling during early organogenesis. Cell 2008;134:921–931
15. Reichert B, Yasmeen R, Jeyakumar SM, et al. Concerted action of aldehyde dehydrogenases influences depot-specific fat formation. Mol Endocrinol 2011;25:799–809
16. De Botton S, Dombret H, Sanz M, et al.; The European APL Group. Incidence, clinical features, and outcome of all trans-retinoic acid syndrome in 413 cases of newly diagnosed acute promyelocytic leukemia. Blood 1998;92:2712–2718
17. Berry DC, DeSantis D, Soltanian H, Croniger CM, Noy N. Retinoic acid upregulates preadipocyte genes to block adipogenesis and suppress diet-induced obesity. Diabetes 2012;61:1112–1121
18. Berry DC, Noy N. All-trans-retinoic acid represses obesity and insulin resistance by activating both peroxisome proliferation-activated receptor beta/delta and retinoic acid receptor. Mol Cell Biol 2009;29:3286–3296
19. Elizondo G, Corchero J, Sterneck E, Gonzalez FJ. Feedback inhibition of the retinaldehyde dehydrogenase gene ALDH1 by retinoic acid through retinoic acid receptor alpha and CCAAT/enhancer-binding protein beta. J Biol Chem 2000;275:39747–39753
20. Ziouzenkova O, Orasanu G, Sharlach M, et al. Retinaldehyde represses adipogenesis and diet-induced obesity. Nat Med 2007;13:695–702
21. Kiefer FW, Vernochet C, O'Brien P, et al. Retinaldehyde dehydrogenase 1 regulates a thermogenic program in white adipose tissue. Nat Med. In press
22. Repa JJ, Hanson KK, Clagett-Dame M. All-trans-retinol is a ligand for the retinoic acid receptors. Proc Natl Acad Sci USA 1993;90:7293–7297
23. Li XH, Kakkad B, Ong DE. Estrogen directly induces expression of retinoic acid biosynthetic enzymes, compartmentalized between the epithelium and underlying stromal cells in rat uterus. Endocrinology 2004;145:4756–4762
24. Wang X, Sperkova Z, Napoli JL. Analysis of mouse retinal dehydrogenase type 2 promoter and expression. Genomics 2001;74:245–250
25. Trasino SE, Harrison EH, Wang TT. Androgen regulation of aldehyde dehydrogenase 1A3 (ALDH1A3) in the androgen-responsive human prostate cancer cell line LNCaP. Exp Biol Med (Maywood) 2007;232:762–771
26. Deiuliis J, Shah Z, Shah N, et al. Visceral adipose inflammation in obesity is associated with critical alterations in tregulatory cell numbers. PLoS ONE 2011;6:e16376
27. Fan X, Molotkov A, Manabe S, et al. Targeted disruption of Aldh1a1 (Raldh1) provides evidence for a complex mechanism of retinoic acid synthesis in the developing retina. Mol Cell Biol 2003;23:4637–4648
28. Rossant J, Zirngibl R, Cado D, Shago M, Giguère V. Expression of a retinoic acid response element-hsplacZ transgene defines specific domains of transcriptional activity during mouse embryogenesis. Genes Dev 1991;5:1333–1344
29. Lasa A, Schweiger M, Kotzbeck P, et al. Resveratrol regulates lipolysis via adipose triglyceride lipase. J Nutr Biochem 2012;23:379–384
30. Oh SA, Suh Y, Pang MG, Lee K. Cloning of avian G(0)/G(1) switch gene 2 genes and developmental and nutritional regulation of G(0)/G(1) switch gene 2 in chicken adipose tissue. J Anim Sci 2011;89:367–375
31. Kim JY, Tillison K, Lee JH, Rearick DA, Smas CM. The adipose tissue triglyceride lipase ATGL/PNPLA2 is downregulated by insulin and TNF-alpha in 3T3-L1 adipocytes and is a target for transactivation by PPARgamma. Am J Physiol Endocrinol Metab 2006;291:E115–E127
32. Haemmerle G, Lass A, Zimmermann R, et al. Defective lipolysis and altered energy metabolism in mice lacking adipose triglyceride lipase. Science 2006;312:734–737

33. Gaidhu MP, Anthony NM, Patel P, Hawke TJ, Ceddia RB. Dysregulation of lipolysis and lipid metabolism in visceral and subcutaneous adipocytes by high-fat diet: role of ATGL, HSL, and AMPK. Am J Physiol Cell Physiol 2010;298:C961–C971
34. Deiuliis JA, Shin J, Bae D, Azain MJ, Barb R, Lee K. Developmental, hormonal, and nutritional regulation of porcine adipose triglyceride lipase (ATGL). Lipids 2008;43:215–225
35. Deiuliis JA, Liu LF, Belury MA, Rim JS, Shin S, Lee K. Beta(3)-adrenergic signaling acutely down regulates adipose triglyceride lipase in brown adipocytes. Lipids 2010;45:479–489
36. Ahmadian M, Abbott MJ, Tang T, et al. Desnutrin/ATGL is regulated by AMPK and is required for a brown adipose phenotype. Cell Metab 2011;13:739–748
37. Caimari A, Oliver P, Palou A. Adipose triglyceride lipase expression and fasting regulation are differently affected by cold exposure in adipose tissues of lean and obese Zucker rats. J Nutr Biochem. In press
38. Yang F, Zhang X, Maiseyeu A, et al. The prolonged survival of fibroblasts with forced lipid catabolism in visceral fat following encapsulation in alginate-poly-l-lysine. Biomaterials 2012;33:5638–5649
39. Ross AC, Cifelli CJ, Zolfaghari R, Li NQ. Multiple cytochrome P-450 genes are concomitantly regulated by vitamin A under steady-state conditions and by retinoic acid during hepatic first-pass metabolism. Physiol Genomics 2011;43:57–67
40. Chen F, Cao Y, Qian J, Shao F, Niederreither K, Cardoso WV. A retinoic acid-dependent network in the foregut controls formation of the mouse lung primordium. J Clin Invest 2010;120:2040–2048
41. Li P, Pashmforoush M, Sucov HM. Retinoic acid regulates differentiation of the secondary heart field and TGFbeta-mediated outflow tract septation. Dev Cell 2010;18:480–485
42. Grove KL, Fried SK, Greenberg AS, Xiao XQ, Clegg DJ. A microarray analysis of sexual dimorphism of adipose tissues in high-fat-diet-induced obese mice. Int J Obes (Lond) 2010;34:989–1000
43. Chen N, Napoli JL. All-trans-retinoic acid stimulates translation and induces spine formation in hippocampal neurons through a membrane-associated RARalpha. FASEB J 2008;22:236–245
44. Poon MM, Chen L. Retinoic acid-gated sequence-specific translational control by RARalpha. Proc Natl Acad Sci USA 2008;105:20303–20308
45. Moenter SM, Chu Z. Rapid nongenomic effects of oestradiol on GnRH neurons. J Neuroendocrinol 2012;24:117–121
46. Moise AR, Lobo GP, Erokwu B, et al. Increased adiposity in the retinol saturase-knockout mouse. FASEB J 2010;24:1261–1270
47. Hessel S, Eichinger A, Isken A, et al. CMO1 deficiency abolishes vitamin A production from beta-carotene and alters lipid metabolism in mice. J Biol Chem 2007;282:33553–33561
48. Zhang M, Hu P, Krois CR, Kane MA, Napoli JL. Altered vitamin A homeostasis and increased size and adiposity in the rdh1-null mouse. FASEB J 2007;21:2886–2896
49. Ström K, Gundersen TE, Hansson O, et al. Hormone-sensitive lipase (HSL) is also a retinyl ester hydrolase: evidence from mice lacking HSL. FASEB J 2009;23:2307–2316
50. Weir JB. New methods for calculating metabolic rate with special reference to protein metabolism. 1949. Nutrition 1990;6:213–221